*Journal of Structural Geology*, Vol 13, No 7, pp 851 to 858, 1991
Printed in Great Britain

0191-8141/91 $03 00+0 00


# Application of digital image analysis in modelling recrystallization processes

CH. JANSSEN, E. BANKWITZ, P. BANKWITZ and G. HARNISCH

Central Institute for Physics of the Earth, Telegrafenberg A 51, 0-1561 Potsdam, Germany

(*Received* 12 *December* 1989; *accepted in revised form* 8 *February* 1991)

**Abstract**—Digital image analysis has been used to interpret the recrystallization processes (grain boundary migration) of rhombohedral camphor which were produced by very low shear deformation in a new Means-type apparatus (Hajeck press). For each stage of shearing the following parameters were computed: grey value distribution of images, area of selected grains and grain shape orientation.

The experimental investigations allow the following conclusions to be made.

(1) Increasing uniformity of grey values (brightness) could be interpreted as indicating that a crystallographic preferred orientation developed during shear deformation.

(2) Extensive increase of grain size and asymmetrical decrease of grain frequency are consequences of grain boundary migration. The alterations took place in several stages.

(3) The grain shapes began changing immediately after the shear deformation started.

The different stages of grain boundary motion (migration) correspond to distinctive physical sources (driving forces) of migration.

## INTRODUCTION

DYNAMIC recrystallization including dynamic recovery is one of the most important processes of rock deformation and has become an object of interest for many geologists. The *in situ* observation of recrystallization behaviour and microstructures during and after experimental deformation of low melting point crystalline material may help us to understand the processes of dynamic recrystallization and recovery as well as of plastic deformation. An experimental technique applicable to simple shearing deformation of samples under microscopic observation has been described by Means & Xia (1981). This Means-type apparatus (Hajeck press) or a modification, was used by several workers (Means & Dong 1982, Means 1983, Jessel 1986, Means & Ree 1988, Stöckhert *et al.* 1988).

All experiments at room temperature show that in low melting point crystalline material, the effects of grain boundary migration without nucleation and the formation of subgrains are dominant. The development of shear zones with consequent adjustment of the shape and size of grains is an additional spectacular feature.

The material used in the experiments described here was camphor. The deformation and dynamic recrystallization of rhombohedral camphor has been described by Urai *et al.* (1980), who discussed mechanisms of dynamic recrystallization and similarity between the behaviour of camphor and minerals of low symmetry.

The aim of this paper is to illustrate the application of digital image analysis in the interpretation of the recrystallization processes during the simple shear of rhombohedral camphor grain aggregates. The application of image processing allows a quantitative interpretation of visual observations.

## EXPERIMENTAL PROCEDURE

Deformation experiments described in this paper were carried out at room temperature using our modification of the Means-type apparatus. The device is mounted on the microscope stage. The preparation of samples between partially frosted glass slides (ordinary thin section glass, Fig. 1) and the following sinistral simple shear deformation is similar to that described by Means & Xia (1981), Means (1983) and Jessel (1986). The glass slides are driven past one another by a motor via a gear box and flexible transmission with a speed between 0.081 and 4.5 mm $min^{-1}$. This corresponds to overall shear strain rates ($\dot{\gamma}$) between $10^{-4}$ and $10^{-6}$ $s^{-1}$ for a sample 10 mm wide. Since deformation is generally inhomogeneous local values are significantly higher or lower.

In our experiments photomicrographs in cross-polarized light were taken about every 30 min during simple shearing at a constant rate ($6.25 \times 10^{-5}$ $s^{-1}$). The photographs (Fig. 2.) show only a small section in the central part of the sample, where the effects of shear strain are low (shear strain rate $\dot{\gamma} = 1.46 \times 10^{-5}$ $s^{-1}$;

Table 1. Conditions of shear deformation

| | |
|---|---|
| Shearing force | 80 N |
| Axial force (normal stress on glass) | 10 N |
| Feed way | 12 mm |
| Rate of feed (shearing speed) | 0.1 mm $min^{-1}$ |
| Temperature | room temp. |
| Duration of experiment | 2 h |
| Time between photographs | 30 min |
| Overall shear strain rate ($\dot{\gamma}$) | $6.25 \times 10^{-5}$ $s^{-1}$ |
| Overall finite shear strain ($\gamma$) | 0.45 |
| Shear strain rate of investigated section ($\dot{\gamma}$) | $1.46 \times 10^{-5}$ $s^{-1}$ |
| Finite shear strain of investigated section ($\gamma$) | 0.10 |

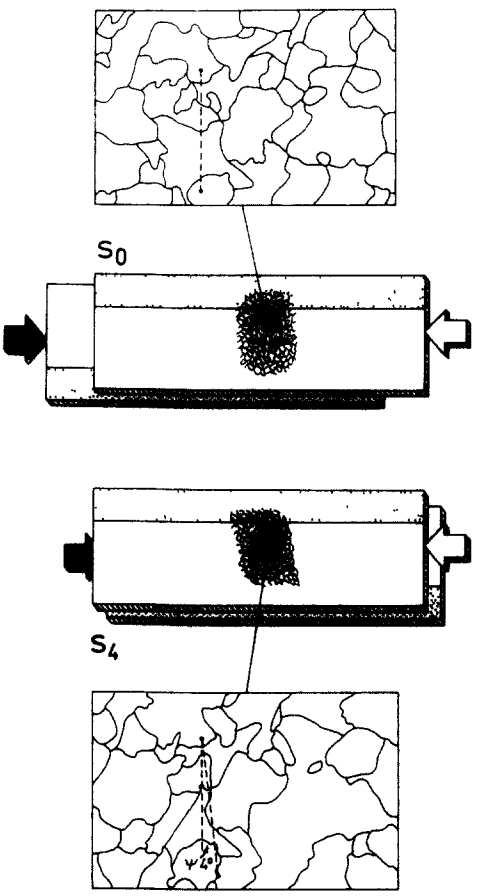


Fig 1 Specimen assembly and grain boundaries prior and after the deformation (two glass slides with frosted grips (dotted) and intervening crystalline camphor) Note. The effects of shear strain are extremely low ($\psi$ = shear angle)

finite shear strain $\gamma = 0.10$) whereas higher strain domains occur adjacent to one of the frosted grips (Fig. 1). A normal stress of 10 N is applied across the plane of the sample by spring clips. The conditions of deformation are presented in Table 1.

Similar experiments with very low and inhomogeneous shear strain have been made in ice (Kamb 1972, Wilson 1986, Burg *et al.* 1986).

## DIGITAL ANALYSIS OF THE PHOTOMICROGRAPHS

To describe the results of the recrystallization experiments quantitatively, methods of image processing were used in a similar way as in other fields, such as biology, medicine and metallography. Applications of image processing and their fundamentals are summarized in Rosenfeld & Kak (1976).

At first the photomicrographs were digitized by the drum scanner FEAG (Kombinat Carl Zeiss Jena). The resulting digital data were evaluated using the image processing system BVS A6472 (Kombinat Robotron Dresden), including eight image memories with a capacity each of 512 × 512 pixel and a pipeline processor. This configuration makes possible fast operations with the contents of the image memories, such as colour encoding, thresholding, filtering, etc

The monitor of the image processing system shows a colour coded picture of the camphor grains. The colours directly depend on the different extinction of the cross-polarized light, which results in turn from the different crystallographic orientation of camphor grains. Therefore the shape of the grey value distribution represents the homogeneity of the crystallographic orientation patterns within the sample But that does not mean that the orientation of the axis of the camphor grains and their strain influenced variation can be detected directly by image processing methods (see below). Therefore the statistics of the orientation of the grain axes was replaced by the statistics of the differential orientation of the grain boundaries. This problem is solved in two steps: (i) extraction of grain boundaries and (ii) statistics of the differential orientation of the boundaries.

Assuming the grains to be represented by areas of more or less homogeneous grey values, the extraction of the grain boundaries is a special case of non-linear filtering. We used the following steps: high-pass-filtering of the original image, thresholding of the high-pass-image, inversion of the grey values and skeletonization of the resulting stripe-like pattern. In this way the original image is transformed into a line pattern representing the grain boundaries. Up to this point the pipeline processor of the image processing system may be used advantageously.

The statistics of the orientation of the grain boundaries is done by line tracing starting at all nodes and free ends of the skeleton. Only the extraction of the starting points may be supported by the pipeline processor, as the following line tracing needs each pixel of the skeleton to be treated separately. The orientation of the skeleton in a given point is derived from the tangent at a parabola through this point and its two neighbours, separated by a given number of pixels. Regarding the geometric properties of digital lines, the distance between the three consecutive points must be three pixels at least. Shifting the three-point-operator over the whole skeleton the orientation of the grain boundaries in each point may be found. The frequency of these values may be presented as a rose diagram, representing in our experiment the strain influenced orientation of the camphor grains.

## EXPERIMENTAL OBSERVATION AND INTERPRETATION

In our experiments, crystal-plastic deformation of camphor grains began with slip, lattice bending and lattice rotation. The lattice rotation led to a change of extinction, reflected by the computer determined alteration of the grey level distribution (i.e. colour change). Therefore Fig. 2 ($S_0 - R$) shows some different grey level distributions (histograms) of the digitalized images which represent several stages of defined shear deformation in one sample The maximum grey value (255)

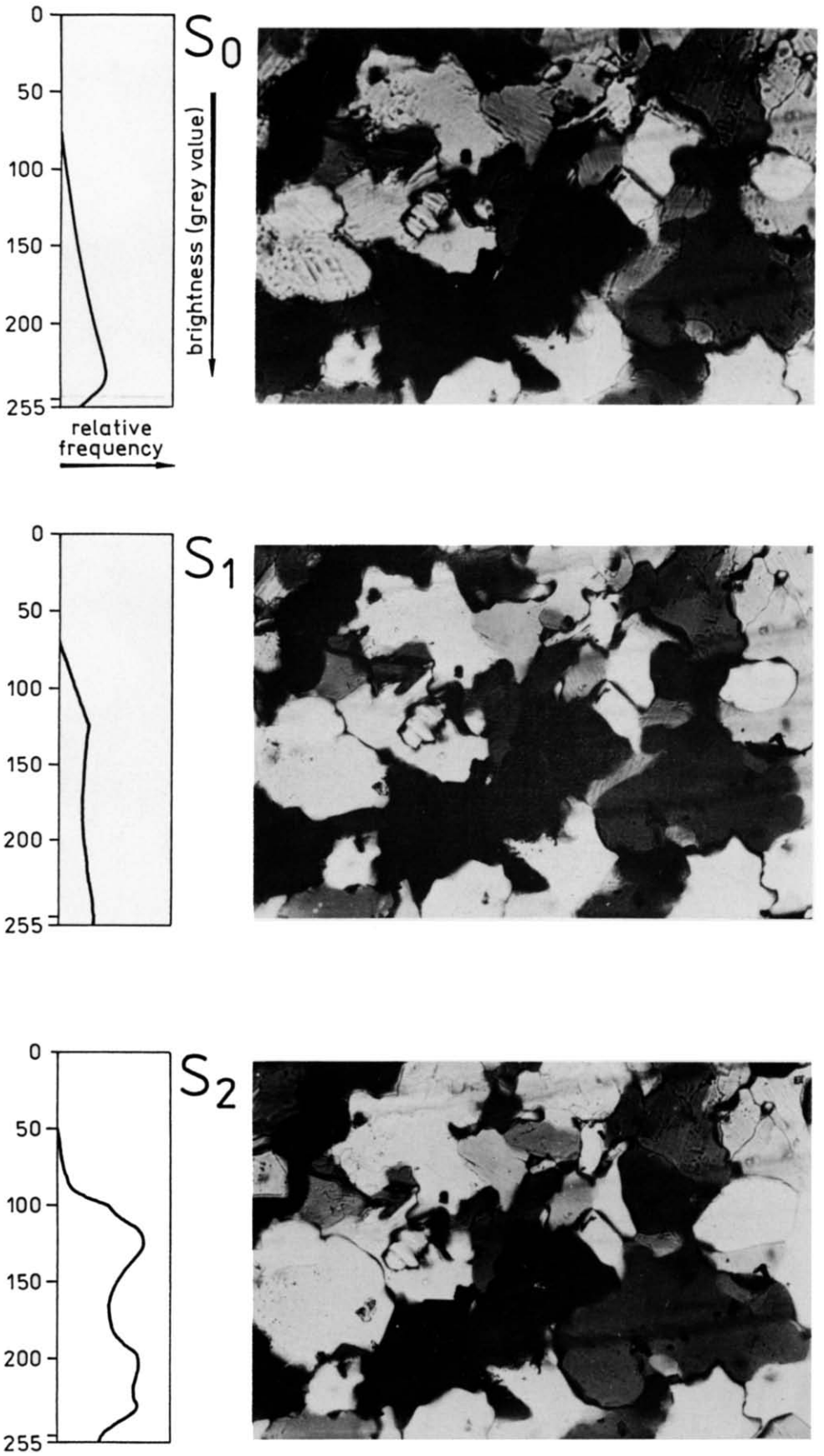


Fig. 2. Histograms of grey level distributions and the corresponding photomicrographs of camphor representing various stages of the shear deformation. $S_0$—immediately before shear deformation (initial stage, $\gamma = 0$); $S_1$–$S_4$—intervals during simple shear deformation (middle stage; $S_1$, $\gamma = 0.11$; $S_2$, $\gamma = 0.21$; $S_3$, $\gamma = 0.32$; $S_4$, $\gamma = 0.45$); $R$—2 h after the end of shear deformation (final stage, after relaxation). Photograph dimensions: 2 mm per side.

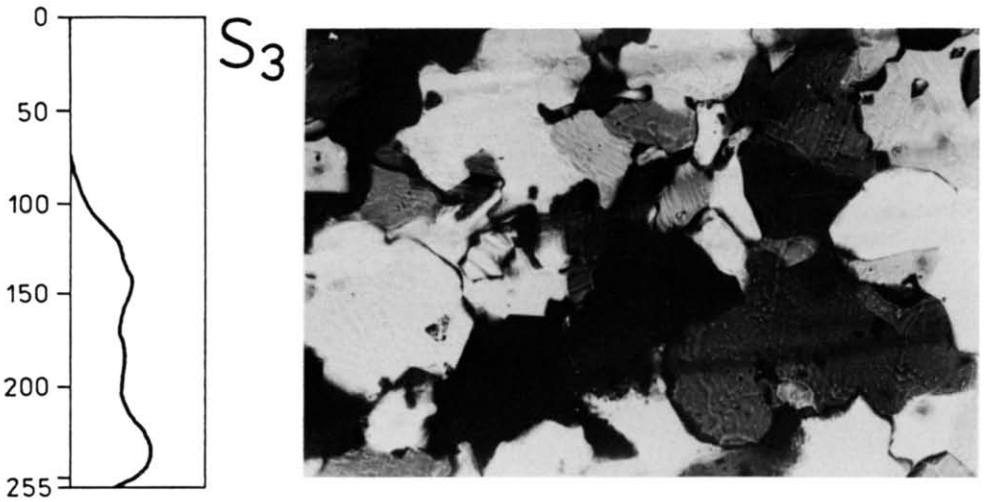


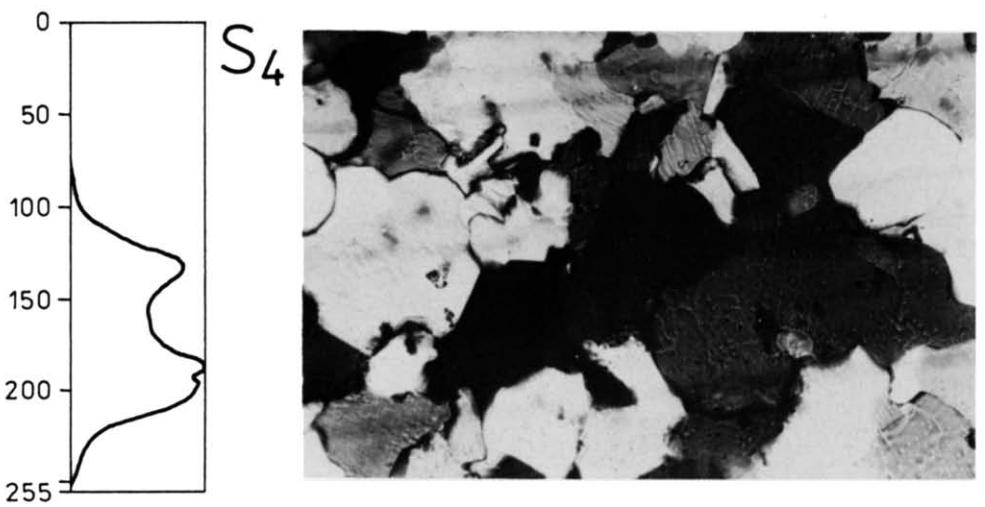


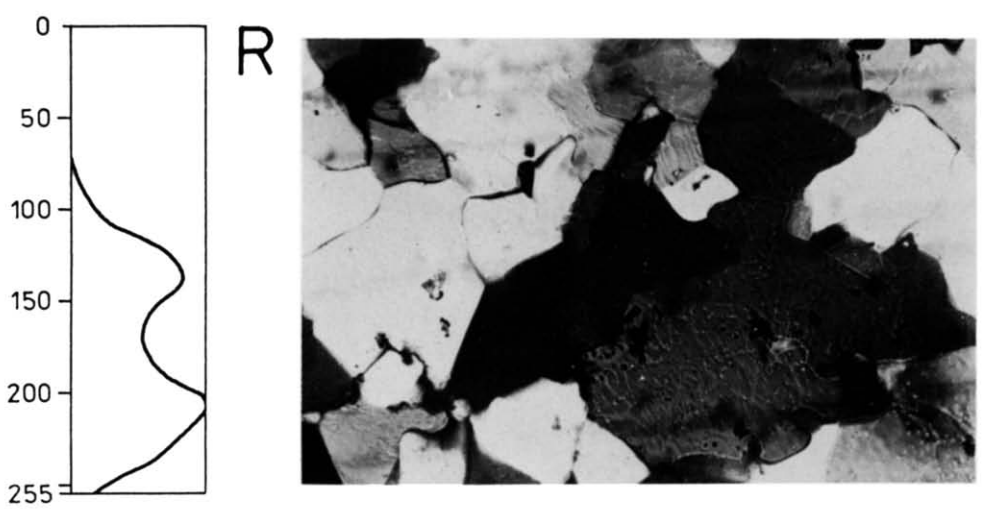


Fig. 2 (*Continued*).

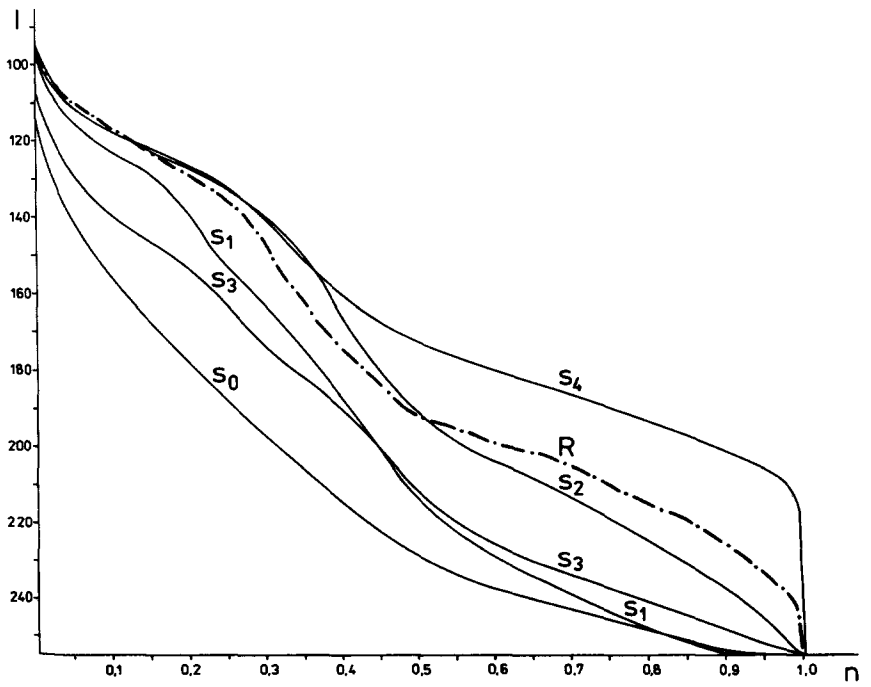


Fig 3 Graph of relative ratio of pixels ($n$) vs intensity of grey value (brightness, $I$). The cumulative curves indicate an advancing uniformity of grey values during shear deformation. $S_0$, $S_1$–$S_4$ and $R$ see explanation, Fig. 2.

corresponds to the greatest possible brightness and vice versa, the minimum grey value (0) corresponds to the greatest possible darkness.

A comparison of several steps of shear deformation indicates an increasing differentiation of the grey level distribution up to the formation of a distribution with two frequency peaks, with the exception of stage $S_3$ (Fig. 2). The cumulative curves (Fig. 3) illustrate the relative frequency of pixels vs grey value intensity (brightness). The increasing brightness (intensity) as an expression of advanced uniformity of grey values could be interpreted as indicating the development of a crystallographic preferred orientation during shear deformation, although the orientation of axes were not determined directly.

Because of our special device, the microscope stage cannot be rotated and tilted about several horizontal axes. Consequently, the direct correlation between the optic orientation of grains and the changes in interference colours as in the Price photometric method (Price 1973, 1980) is impossible. But the advantage of our method compared with Price's method is the higher information content of the measured light intensity. According to Price the spectrum for an aggregate of $n$ mineral grains is the weighted linear sum of individual grain spectra, whereas by using digital image analysis the local transmission intensity of every grain is detected.

It is apparent that stage $S_3$ represents an exception. An increase of darkness is characteristic for the relaxation phase. These varying developments, also reflected by grain size distribution and changes of grain shapes (see below), probably results from grain boundary migration (GBM) with different driving forces.

Grain boundaries begin to migrate by shifting of high-angle crystal boundaries immediately after the start of shearing, too. Figures 2 ($S_0$ – $R$), 4 and 5 show this migration during different stages of shear deformation. Grain boundaries were already serrated and rugged before the initial stages of shearing (Figs. 2, $S_0$, and 5a). Therefore, a weak initial strain should have been introduced into the material, as a result of sample preparation. The following shear deformation produced only a very low longitudinal strain ($R_s$ 1.52), estimated by the two-dimensional strain analysis ($R_f$ method) parallel to the $XY$-plane in the centre of the sample.

Selected marker particles picked up by the photos were used to check the small change of the configuration (distances and angles) in the centre (Figs. 6a & b). The sense of movement of all markers is equal (Fig. 6c), only differing with their angles related to the $c$-plane.

During sustained shearing, grain boundary migration continued and led to an increase of the average grain size and a reduction of the similar lattice orientations and consumption of intervening grains (Figs. 4 and 5d). The estimation of grain size has been carried out also by digital image processing analysis. A computer program counts and stores the pixels inside of grain contours. Figure 7 shows the results of calculation with regard to the different stages of deformation. It is easy to recognize that a quantitative increase of average grain size exists. The larger grains tend to grow at the expense of smaller ones. But the growth rate is not constant with time for each grain, and not identical for all grains. We suppose that this fact depends on the more or less favourable orientation of the lattice slip planes for gliding. After significant alteration of grain size in the first stage, no changes of grain size have been observed in the middle stage. The increase of grain size in the last stage results from coalescence with neighbouring grains.

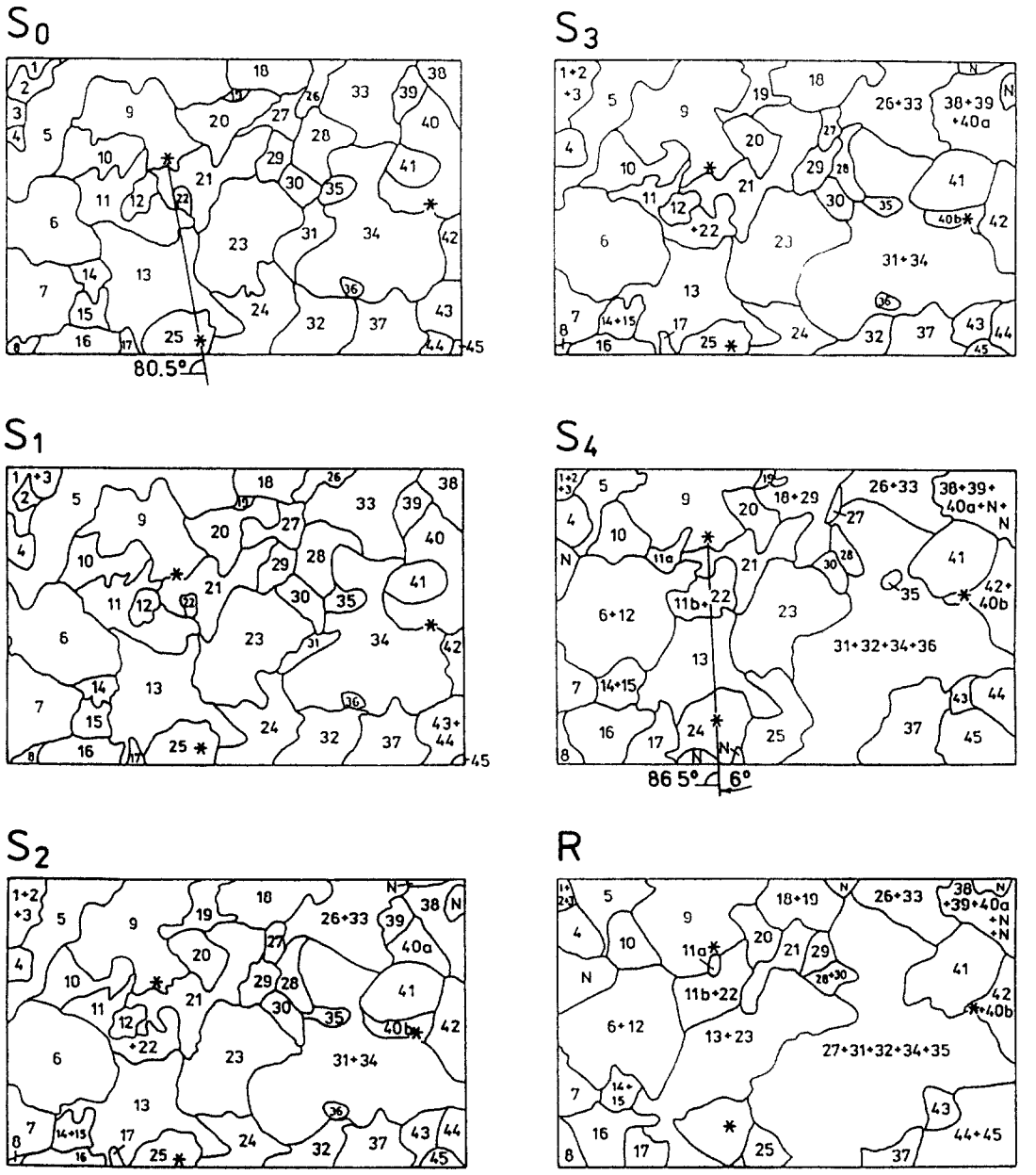


Fig 4. Maps of one camphor sample show grain boundary migration before ($S_0$), during ($S_1$–$S_4$) and after ($R$) shear deformation. Map dimensions. 2 mm per side

We believe that the different increases of grain size are controlled by various physical sources of grain boundary migration (see Conclusions). Moreover, it becomes obvious that the boundaries migrate toward their respective centres of curvature with the result that they become increasingly straight, especially in the final stage (Fig. 5a).

Rose diagrams derived from the grain boundaries before, during and after the shear deformation are shown in Fig. 8. It is suggested that the development of grain shape changes began immediately after the start of shear deformation.

After each experiment (duration of experiments is 2 h) the samples were unloaded and relaxation was achieved, reflected by extensive grain growth at room temperature. Two hours later, the average grain size was larger than at any stage in the shear deformation (Figs. 2 $S_6$, and 4). The features of grain boundaries after their relaxation remind us of secondary recrystallization (in spite of different recrystallization mechanisms) characterized by extremely large growth of only a few grains at the expense of others (Poirier 1985).

## DISCUSSION AND CONCLUSIONS

The conspicuous process in these simple-shear experiments, carried out at room temperature, is grain boundary migration. The significant grain boundary migration, of the type that produces very irregular, wavy, or serrated grain boundaries, can go on independently of any large concurrent deformation. Migration took place at different steps and places of grain boundaries. Periods of relative repose will be relieved by phases of conspicuous change, whereby the greatest changes have been ob-

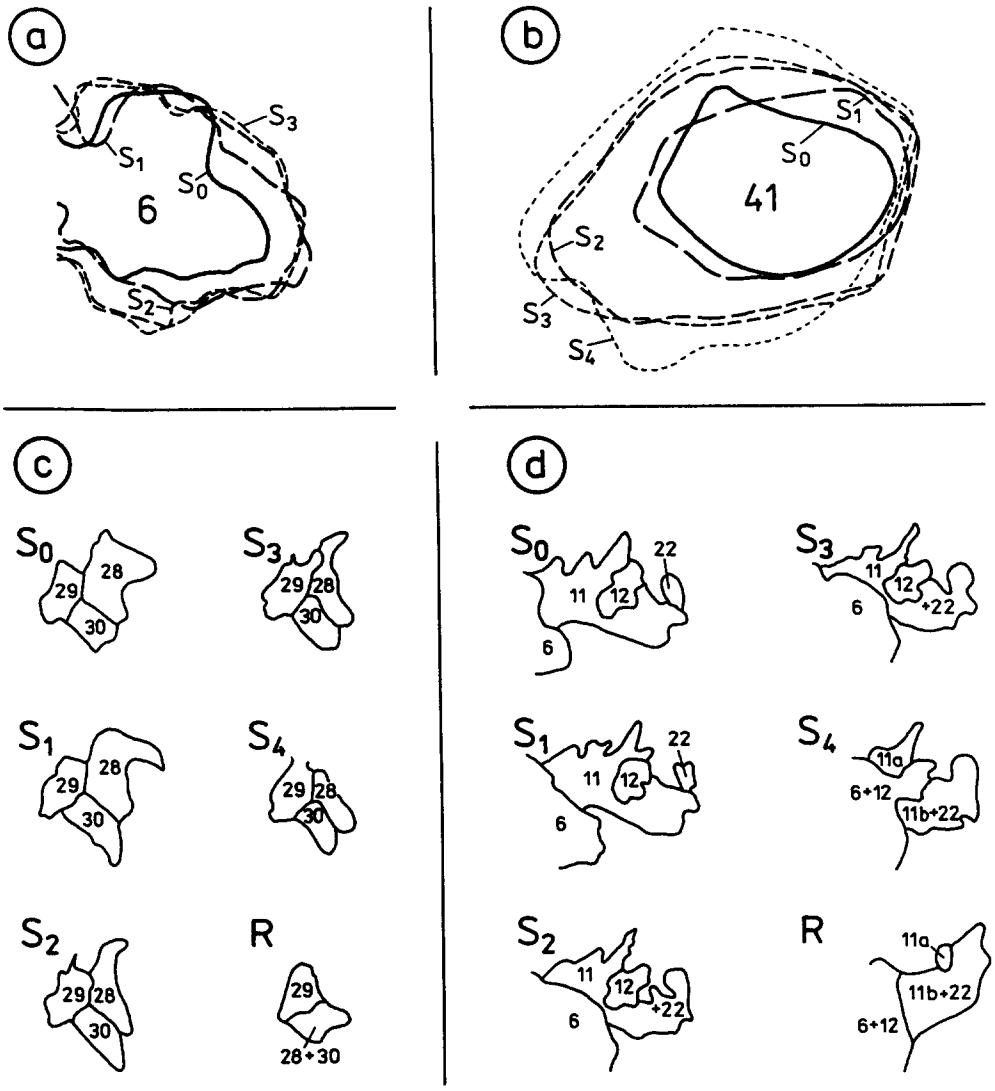


Fig. 5. Detailed graphs of grain boundary motion. (a) & (b) Grain boundary migration during shear deformation; (c) & (d) examples of grain dissection.

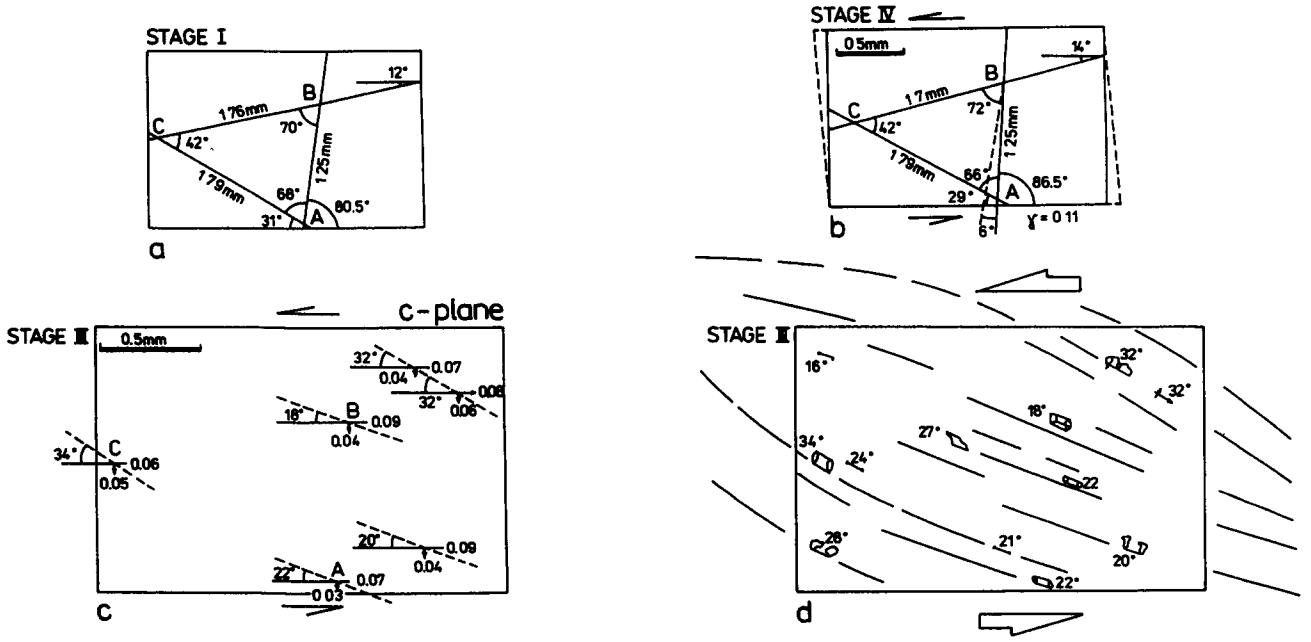


Fig. 6. Results of the sinistral shear experiment in the centre of the sample. Measurements made on markers seen in the photographs were used to define the displacements and changes in angles produced by the small deformation (a) Angular relationships and distances of three particles (A, B and C) in the initial state. (b) The configuration in the final state. (c) Displacements (in mm) and orientations of the particle displacement trajectories for some individual markers in stage $S_3$. (d) Overall pattern of particle displacement trajectories determined from several selected markers.

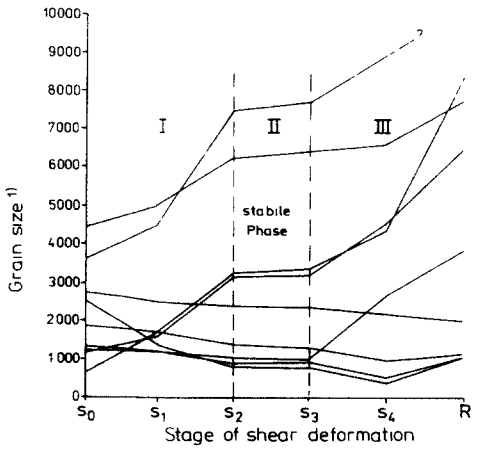


Fig 7 Development of grain size (individual grains) in dependence on shear strain I—initial stage, II—middle stage, III—final stage; $S_0$, $S_1$–$S_4$ and $R$ see explanation Fig. 2. (1) Pixels under and inside of grain contour (line pattern that represents the grain boundaries)

served immediately after the beginning of shear deformation and during relaxation.

The driving force for this migration is not known, exactly. The developments of grey level distribution, grain size, grain shape and grain orientation derived by methods of digital image processing suggest several stages during the recrystallization process. The significant middle stage is characterized by stability of grain size (stable phase) as well as by a decrease of grey values and of differentiation of grey level distribution Consequently, the assumption is made here that the several stages correspond to different driving forces of recrystallization. In most of the known deformation experiments with boundary migration the difference in dislocation density (and specific free energy) between the grains is the driving force for migration (strain-induced boundary migration/SIBM, Poirier 1985) But in our experiment, the stored energy of grains as a result of the very low shear strain is not high enough to produce grain boundary migration in the early stages of deformation. Consequently, at the beginning of deformation, the stress-induced boundary migration (difference in elastic strain energy between two grains/elastic deformation; Poirier 1985) in consequence of sample preparation is more probably dominant. During the later stages of deformation the difference in lattice defect energy grows and so the importance of strain-induced boundary migration may increase.

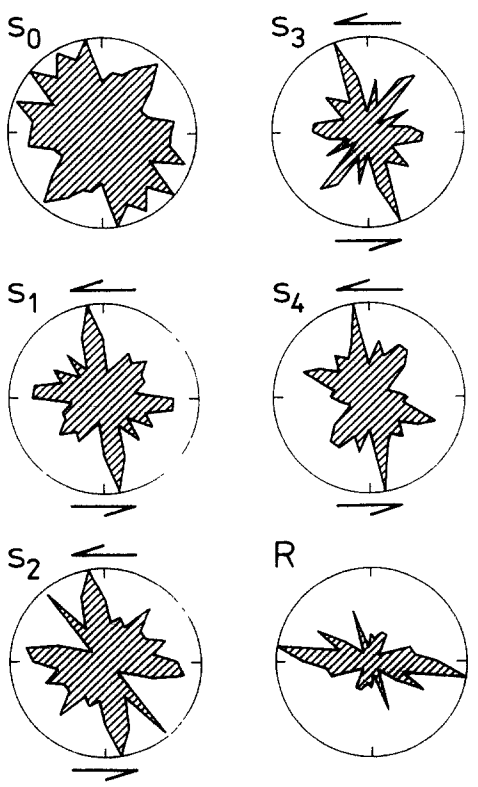


Fig 8 Rose diagrams with grain shape orientations $S_0$, $S_1$–$S_4$ and $R$ see explanation, Fig 2

*Acknowledgements*—The authors thank Dr Means and Dr Riedel for kind support, and Dr Schilbach for help in using his computer programs. Critical reviews and helpful comments by M W. Jessel and an anonymous referee substantially improved the manuscript

## REFERENCES

Burg, J P , Wilson, C J L & Mitchell, J C 1986 Dynamic recrystallization and fabric development during simple shear deformation of ice. *J Struct Geol* **8**, 857–870

Jessel, M W 1986. Grain boundary migration and fabric development in experimentally deformed octochloropropane *J Struct Geol* **8**, 527–542

Kamb, W B 1972 Experimental recrystallization of ice under stress In *Flow and Fracture of Rocks* (edited by Heard, H C , Borg, I. Y , Carter, N L & Raleigh, C B ) *Am Geophys Un Geophys Monogr* **16**, 211–241

Means, W D 1983. Microstructure and micromotion in recrystallization flow of octochloropropane· a first look *Geol Rdsch* **72**, 511–528

Means, W D & Dong, H 1982 Some unexpected effects of recrystallization on the microstructures of material deformed at high temperature *Mitt Geol Inst ETH, Neue Folge* **239a**, 205–207

Means, W. D & Xia, Z G. 1981 Deformation of crystalline materials in thin section *Geology* **9**, 538–543

Means, W D & Ree, J H. 1988 Seven types of subgrain boundaries in octochloropropane *J Struct Geol* **10**, 765–770

Nega, H & Janssen, Ch In press. Schervorrichtung fur mikroskopische Untersuchungen an plastischen Substanzen *Z geol. Wiss* **18**

Poirier, J P 1985 *Creep of Crystals* Cambridge University Press, Cambridge

Price, G P 1973 The photometric method in microstructural analysis *Am. J Sci.* **273**, 523–537

Price, G P 1980 The analysis of quartz *c*-axis fabrics by the photometric method *J Geol* **88**, 181–196

Rosenfeld, A & Kak, A C 1976 *Digital Picture Processing* Academic Press, New York

Stockhert, B , Hucke, M , Rosner, G. & Harbott, W 1988 Experimental deformation of low melting point crystalline material under the polarizing microscope—experiences with a new Means type apparatus. *Terra Cognita* **8**, 78

Urai, J L , Humphreys, F J. & Burrows, S E 1980 *In situ* studies of deformation and dynamic recrystallization of rhombohedral camphor *J Mater Sci* **15**, 1231–1240

Wilson, C J L 1986 Deformation induced recrystallization of ice the application of *in situ* experiments In· *Mineral and Rock Deformation—Laboratory Studies* (edited by Hobbs, B. E & Heard, H C ). *Am Geophys. Un. Geophys Monogr.* **36**, 213–232